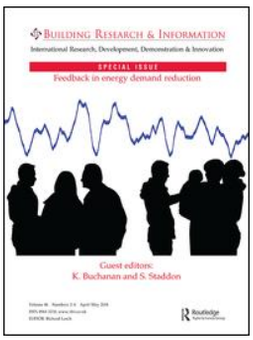

Routledge
Taylor & Francis Group

Building Research & Information

ISSN: 0961-3218 (Print) 1466-4321 (Online) Journal homepage: https://www.tandfonline.com/loi/rbri20

Internal surface condensation risk in façades of Spanish social dwellings

David Bienvenido-Huertas, Carlos Rubio-Bellido, Daniel Sánchez-García & Juan Moyano

To cite this article: David Bienvenido-Huertas, Carlos Rubio-Bellido, Daniel Sánchez-García & Juan Moyano (2019): Internal surface condensation risk in façades of Spanish social dwellings, Building Research & Information, DOI: 10.1080/09613218.2019.1612729

To link to this article: https://doi.org/10.1080/09613218.2019.1612729

BUILDING RESEARCH & INFORMATION
2019
https://doi.org/10.1080/09613218.2019.1612729

Internal surface condensation risk in façades of Spanish social dwellings

David Bienvenido-Huertas [a], Carlos Rubio-Bellido [b], Daniel Sánchez-García [b] and Juan Moyano [a]

[a]Department of Graphical Expression and Building Engineering, University of Seville, Seville, Spain; [b]Department of Building Construction II, University of Seville, Seville, Spain

ABSTRACT

The poor maintenance of social dwellings causes the possible building deficiencies to be significantly increased, especially when most of these dwellings have been built before any thermal standard and without considering the effect of climate change. Façades are one of the building elements which are most degraded by the contact with the exterior, and surface condensation is the most common cause. This study applies the calculation of surface condensation from ISO 13788 to a representative case of social dwelling in Spain for all climate zones, both in the current and 2050 scenarios. Risks of corrosion, mould formation, and surface condensation were studied in nine different points of the façade, which were validated by *in-situ* measurements. The results determined that there was a greater risk of condensation or mould depending on the climate zone, and thermal resistance significantly influenced data variation in future scenarios. The results also showed that an adequate ventilation generally decreased risks, removing the risk of mould and surface condensation by 2050. To predict the results obtained, a model based on artificial neural networks was generated, and it could also be used to estimate risks in the future.

ARTICLE HISTORY
Received 9 January 2019
Accepted 25 April 2019

KEYWORDS
Climate change; climate zones; internal surface condensation; multi-layer perceptron; simulation

Introduction

The lack of building maintenance plans can contribute to the progressive degradation of buildings. Façades are among those building elements that tend to be most affected by the lack of maintenance. The interaction of the façade with the exterior results in degradation due to factors such as rain and humidity (Orr, Young, Stelfox, Curran, & Viles, 2018; Pereira, de Brito, & Silvestre, 2018). One of the most typical causes of degradation of brick façades is surface condensations. From areas with mild winters to areas with severe winters (Becker & Jaegermann, 1982; Torres-Rivas et al., 2018), there are many cases of degradation caused by surface condensation. Condensation occurs when the internal surface temperature of an element is lower than the dew-point temperature (Bellia & Minichiello, 2003). In a façade, the areas contributing to this effect are thermal bridges (*e.g.* slab fronts and windows), although condensations can also occur in other areas (Bellia & Minichiello, 2003), thus affecting their thermal properties (Barreira & de Freitas, 2013).

The appearance of surface condensation depends on several factors, such as temperature and humidity (Urquhart, 1982), the kind of material (Gradeci, Labonnote, Time, & Köhler, 2017), the size of the surface area of the façade (Hens, 2003), and the room volume (Woolliscroft, 1997). Although cold climate conditions can imply the appearance of surface condensation problems, such problems are more likely in moderate climate zones due to both deficient heating patterns and the low thermal insulation of the buildings in such zones (Becker, 1993). In this sense, poor internal air ventilation significantly influences the condensation risk. Ventilation in the existing building stock is deficient in most cases, thereby causing the appearance of surface condensation (Dimitroulopoulou, 2012). The influence of user's behaviour can also lead to condensation. The difficulties to raise users' awareness of the importance of a correct ventilation make the obtaining of solutions to this problem quite challenging (Levie et al., 2014; Sharpe, Bearman, Thornton, Husk, & Osborne, 2015). The ventilation of bedrooms is a good example. The air change rate of bedrooms is low in winter nights in most regions to maintain adequate thermal comfort conditions (Hou et al., 2018). Such inadequate ventilation increases the surface condensation risk in this season (Liu, Aizawa, & Yoshino, 2004). Having ventilation systems would reduce condensation by 20% (Liu et al., 2004), although this data could not be extrapolated to all regions.

CONTACT David Bienvenido-Huertas jbienvenido@us.es

Likewise, fuel poverty also encourages the appearance of surface condensation problems (Galvin & Sunikka-Blank, 2017; Sharpe, Thornton, Nikolaou, & Osborne, 2015). Inadequate warming in turn implies deficient hygrothermal conditions, thus encouraging surface condensations on building elements (Sharpe, Bearman, et al., 2015).

Furthermore, mould growth can be a problem for users' health. If there are not acceptable dry conditions, water content is maintained in walls during long periods of time. This excess humidity on the internal surface encourages mould growth (Krus, Rosler, & Sedlbauer, 2006), which sheds spores to the internal environment (Emenius, Egmar, & Wickman, 1998). The presence of mould in buildings is a very common aspect in various countries: (i) in a study performed by Platt, Martin, Hunt, and Lewis (2009), mould was detected in 45.9% of the 597 British dwellings analysed; (ii) in another similar study by Koskinen, Husman, Meklin, and Nevalainen (1999), a sample of 310 houses were analysed in Finland. The results showed that 52% of dwellings presented humidity problems and 27% had mould problems; and (iii) Howden-Chapman, Saville-Smith, Crane, and Wilson (2005) examined 613 dwellings in New Zealand. The authors noticed that 46.5% of dwellings had visible mould in rooms. There are several research studies showing the existing correlation between the formation of mould and the appearance of allergy symptoms (Holme, Hägerhed-Engman, Mattsson, Sundell, & Bornehag, 2010; Jacob et al., 2002). This aspect becomes important taking into account that users are inside their dwelling for a long time (Schweizer et al., 2007). The reduction of the condensation risk therefore helps to ensure better indoor air quality (IAQ), which in turn avoids health problems (Gładyszewska-Fiedoruk, 2013).

The method to determine the condensation risk is included in ISO 13788 (International Organization for Standardization, 2012). It is a theoretical method which uses monthly data of temperature and humidity. In the scientific literature, however, there are other methods to estimate the surface condensation risk: (i) Liu et al. (2004) developed a three-dimensional model using computational fluid dynamics to simulate surface condensations in a test chamber. The results presented an adequate degree of adjustment with respect to the experimental results; (ii) Klemm, Klemm, Rozniakowski, and Wojtatowicz (2002a, 2002b) used a method to measure surface condensations by applying laser radiation. The results showed a great correlation between the roughness of the element and the mould growth; (iii) Antonyová et al. (2013) developed a non-destructive method to measure the condensation on walls. This method was used in two buildings in Slovakia, and the results were similar to those obtained by simulation; and (iv) Haldi (2015) devised a method that estimated the risk of humidity in the interior. For this purpose, stochastic models based on users' behaviour were used.

Also, there are research works analysing surface condensations on buildings in various regions, thereby allowing this problem to be characterized: (i) Becker (1984) analysed the influence of the orientation, occupation, and habits in the risk of mould growth in 200 dwellings. The results reflected that buildings facing north presented a condensation risk greater than those facing other orientations (due to the lack of solar contributions). In addition, the inadequate ventilation and a high number of people in the dwelling contributed to an increase of the condensation risk; (ii) a study carried out by the Building Research Establishment (BRE) (Dimitroulopoulou et al., 2005) determined that 68% of the dwellings built in United Kingdom since 1995 had an air change rates lower than 0.5, thus implying a risk of surface condensation in winter; (iii) another study conducted in United Kingdom showed that the methodology used to evaluate the heat transfer in windows can underestimate the risk of mould growth on walls (Sierra, Bai, & Maksoud, 2015); (iv) Bekö, Lund, Nors, Toftum, and Clausen (2010) analysed the air change rate in 500 bedrooms of Danish children between 3 and 5 years old. The results showed a correlation between the surface condensation on windows and the low air change rate; (v) Shin, Rhee, Lee, and Jung (2018) evaluated the CO_2-based ventilation control in two residential buildings in Korea. The results allowed the surface condensation risk to be reduced even for external temperatures of −15°C; (vi) Kim, Kim, and Leigh (2011) studied the use of a double window system with ventilation slits to reduce the surface condensation risk in apartments in Korea. Such system both decreased the internal humidity by 50% and removed surface condensations from window frames; (vii) Cho, Iwamoto, and Kato (2016) analysed the possibilities of decrease in an office building located in Tokyo. By incorporating great thicknesses of insulation materials (greater than 7.5 cm) and triple float glass windows, condensation risks were removed; and (viii) Dallongeville et al. (2015) studied the IAQ in 150 dwellings in France. The results reflected concentrations of different kind of mould, such as *Cladosporium* and *Penicillium*, in more than 90% of dwellings.

However, there is a lack of research studies analysing internal condensation risks in the Spanish building stock. Spain is characterized by having a wide typology of climate zones (Peci López & Ruiz de Adana Santiago, 2015), which goes from desert climate (Bw) to subarctic climate (Dsc), according to the Köppen-Geiger climate

classification (Rubel & Kottek, 2010). In addition, most of the building stock was built without any technical quality standard in the building sector (Kurtz, Monzón, & López-Mesa, 2015). In this regard, 54.71% of social dwellings of the existing building stock was built in Spain in the 20th century (between 1940 and 1979). This dwelling typology is characterized by having façades with low thermal resistance as well as by not having ventilation systems (Kurtz et al., 2015).

This study therefore aims at analysing the surface condensation risk in the existing social dwellings in Spain. To do this, a representative case study was selected, and the appearance of surface condensation was evaluated according to the climate zone. Environmental conditions (internal operative temperature and internal relative humidity) were simulated using DesignBuilder, and internal surface temperatures of the façade were simulated with HTflux, using models validated by *in-situ* measurements. The effect of having ventilation systems was also assessed. Given that the Directive 2018/844 (European Union, 2018) established the need for having efficient buildings before 2050, the existing condensation risk in buildings which are not renovated in that year has also been analysed. Finally, automation tools were developed by using artificial neural networks (ANNs) to ease the analysis in future research studies.

Method

The methodological frame of this research is based on the selection of a representative case study of Spanish social dwellings from the 20th century. After selecting the case study, climate zones were characterized both in the current scenario and 2050. Afterwards, the case study was modelled, validated, and the data required were simulated, from which conclusions were drawn. Furthermore, data were used as training and validation datasets for the ANNs.

Theory and calculation method

ISO 13788 (International Organization for Standardization, 2012) establishes a calculation method to evaluate problems related to the surface condensation of building envelope elements. For this purpose, the concept of temperature factor at the internal surface ($f_{R_{si}}$) is introduced:

$$f_{R_{si}} = \frac{T_{s,\mathrm{in}} - T_{\mathrm{out}}}{T_{\mathrm{in}} - T_{\mathrm{out}}}, \tag{1}$$

where $T_{s,\mathrm{in}}$ [°C] is the internal surface temperature of the element, T_{in} [°C] is the internal operative temperature, and T_{out} [°C] is the external dry bulb temperature.

By using Equation (1), two different $f_{R_{si}}$ can be obtained: (i) the $f_{R_{si}}$ presented by the element at the instant analysed. The surface temperature can be determined by methods of finite elements according to ISO 10211 (International Organization for Standardization, 2017); and (ii) the limit $f_{R_{si}}$ which will determine the condensation risk. To obtain this last $f_{R_{si}}$, it is necessary to determine both the saturation pressure (p_{sat}) and the limit internal surface temperature related to that pressure ($T_{s,\mathrm{in,limit}}$). Equations (2)–(4) indicate how they can be obtained. Values of $f_{R_{si}}$ of the element higher than the limit $f_{R_{si}}$ will not present surface condensation risks.

$$p_{\mathrm{sat}} = \frac{p_{\mathrm{in}}}{\varphi_{si,cr}}, \tag{2}$$

$$T_{s,\mathrm{in,limit}} = \frac{237.3 \cdot \log_{\mathrm{e}}\left(\frac{p_{\mathrm{sat}}}{610.5}\right)}{17.269 - \log_{\mathrm{e}}\left(\frac{p_{\mathrm{sat}}}{610.5}\right)} \tag{3}$$

$$\text{for } p_{\mathrm{sat}} \geq 610.5 \text{ Pa},$$

$$T_{s,\mathrm{in,limit}} = \frac{265.5 \cdot \log_{\mathrm{e}}\left(\frac{p_{\mathrm{sat}}}{610.5}\right)}{21.875 - \log_{\mathrm{e}}\left(\frac{p_{\mathrm{sat}}}{610.5}\right)} \tag{4}$$

$$\text{for } p_{\mathrm{sat}} < 610.5 \text{ Pa},$$

where p_{in} [Pa] is the internal pressure, and $\varphi_{si,cr}$ [dimensionless] is the critical relative humidity. To determine the value of $\varphi_{si,cr}$, the standard suggests the use of three values for three types of surface condensation risks: corrosion of metal elements ($\varphi_{si,cr}$ is 0.6), mould growth ($\varphi_{si,cr}$ is 0.8), and surface condensation ($\varphi_{si,cr}$ is 1.0).

The standard uses monthly mean values with the aim of simplifying the calculation procedure. However, this analysis presents limitations because the condensations generated during the most unfavourable hours are not detected. Therefore, the approach from ISO 13788 was applied at a schedule level to have greater information about the surface behaviour of the building envelope.

Case study

A residential building built in 1978 in Seville was selected (see Figure 1(a)) because it represents most existing residential buildings in the country. According to data from the Housing Census in Spain (Spanish Institute of Statistics, 2011), 54.71% of social dwellings of the existing building stock were built between 1941 and 1980. This period corresponds to the period before publishing the NBE-CT 79 standard (The Government of Spain, 1979), which establishes the quality criteria of the building energy behaviour, such as the incorporation of insulation material in façades. This case study is therefore

(a) (b)

Figure 1. Case study: (a) façade of the building, and (b) 3D model of the room.

representative of a high percentage of the building stock in Spain, as well as corresponds to buildings in which performances and improvements should be made to reduce the energy consumption and increase comfort and healthiness conditions (Kurtz et al., 2015).

These buildings present an inadequate equilibrium between the generation and removal of humidity due to poor ventilation, thereby having acceptable conditions to cause surface condensation problems. The dwellings have six rooms with different orientations. For this study, the most unfavourable case was analysed: the bedroom facing north (see Figure 1(b)). In such types of rooms this is where most humidity appears, especially at night (Shin et al., 2018). Likewise, these rooms are only ventilated with windows, so the condensation risk is higher due to the lack of users' awareness (Levie et al., 2014; Park & Kim, 2012). The room studied is only used by one user, a student, who is studying and sleeping in the room most of the time.

Climate zones

Spain is a country with a wide variety of climate zones. The various areas are classified by using the Spanish Building Technical Code (CTE) (The Government of Spain, 2013). This method uses the concepts of winter climate severity (WCS) and summer climate severity (SCS).

$$\mathrm{WCS} = 3.546 \cdot 10^{-4} \cdot \mathrm{DD}_W - 4.043 \cdot 10^{-1} \cdot \frac{n}{N} + 8.394 \cdot 10^{-8} \cdot \mathrm{DD}_W^2 - 7.325 \cdot 10^{-2} \cdot \left(\frac{n}{N}\right)^2 - 1.137 \cdot 10^{-1}, \quad (5)$$

$$\mathrm{SCS} = 2.990 \cdot 10^{-3} \cdot \mathrm{DD}_S - 1.1597 \cdot 10^{-7} \cdot \mathrm{DD}_S^2 - 1.713 \cdot 10^{-1}, \quad (6)$$

where DD_W is the mean degree days, based on 20°C in winter (between October and May); n/N is the quotient between the number of sunny hours (n) and the number of maximum sunny hours (N) between October and May; and DD_S is the mean degree days, based on 20°C in summer (between June and September).

Each region is classified according to the WCS and SCS values obtained. For WCS, a letter between A and E is assigned, and for SCS, a number between 1 and 4 (see Table 1). By combining WCS and SCS in each of the Spanish province capitals, 12 different climate zones are obtained (see Figure 2). In this study, a city representing each climate zone was analysed (see Table 2). EnergyPlus Weather (EPW) files of each climate zone in the current scenario were generated from MET files of the CTE (The Government of Spain, 2017).

Scenario 2050

To generate future climate scenarios, 12 EPWs of the current scenario were selected. A morphing process was applied to these files with the UK Met Office Hadley Centre Coupled Model 3 HadCM3 (Met Office Hadley Centre, 2016). This model considers the combination of scenarios of CO_2 A2a, A2b, and A2c emissions, forming the GHG A2 emissions scenario. By using the tool called CCWorldWeatherGen (Jentsch, Bahaj, & James, 2008; Jentsch, James, Bourikas, & Bahaj, 2013), which is based on research studies by Belcher, Hacker, and Powell (2005), the climate files for 2050 were created

Table 1. Intervals of classification for WCS and SCS.

Intervals for WCS		Intervals for SCS	
Class	**Value**	**Class**	**Value**
A	$0 \leq WCS \leq 0.23$	1	$SCS \leq 0.50$
B	$0.23 < WCS \leq 0.50$	2	$0.50 < SCS \leq 0.83$
C	$0.50 < WCS \leq 0.93$	3	$0.83 < SCS \leq 1.38 SCS \leq 0.50$
D	$0.93 < WCS \leq 1.51$	4	$SCS > 1.38$
E	$WCS > 1.51$		

(*i.e.* the time series of the climate variables for 2050). The 12 EPW files were therefore morphed, obtaining 12 new climate scenarios for 2050.

Although the HadCM3 A2 model is the most widely used to perform simulations for future predictions (Jentsch et al., 2013) and several research studies are based on this model (Bienvenido-Huertas, Moyano, Rodríguez-Jiménez, & Marín, 2019), some considerations are required. The HadCM3 model has a grid resolution of $2.5 \times 3.8°$ (Pope, Gallani, Rowntree, & Stratton, 2000), which means that each simulated grid element should cover around 278×422 km, thus allowing predictions to be carried out to the scale of climate zones from Table 2. For specific case studies, however, the model presents certain level of uncertainty. Moreover, it predicts future tendencies of the climate variables, but it cannot contemplate extraordinary natural phenomena related to climate change, such as hurricanes, storms, strong seasonal floods, etc. The 2050 future scenario used in this research should be understood as the most probable climate conditions in the future, considering the A2 'medium-high' GHG emissions scenario with a margin of error corresponding to the size of the grid of the HadCM3 model.

Table 2. The cities selected for each climate zone.

Climate zone	City	Latitude	Length	Height
A3	Malaga	36.67	−4.48	7.0
A4	Almeria	36.85	−2.38	21.0
B3	Murcia	38.00	−1.17	62.0
B4	Seville	37.42	−5.90	31.0
C1	Bilbao	43.30	−2.90	39.0
C2	Barcelona	41.28	2.07	6.0
C3	Granada	37.18	−3.78	570.0
C4	Caceres	39.47	−6.33	405.0
D1	Oviedo	43.35	−5.87	339.0
D2	Girona	41.90	2.77	129.0
D3	Albacete	38.95	−1.85	704.0
E1	Soria	41.81	−2.65	1079.0

The 2050 scenario significantly influences the climate variables of the EPW files. Generally, the annual average temperature had increases greater than 4°C, although such increase was not the same throughout the year: the coldest months (*e.g.* January and February) had a temperature increase lower than the hottest months (*e.g.* July and August). Concerning the variation of the external relative moisture, it presented decreases in all months of the year. In this way, the average variation with respect to the current scenario throughout the year was 2%, with the exception that the deviation oscillated between 13.8 and 15.9% in July.

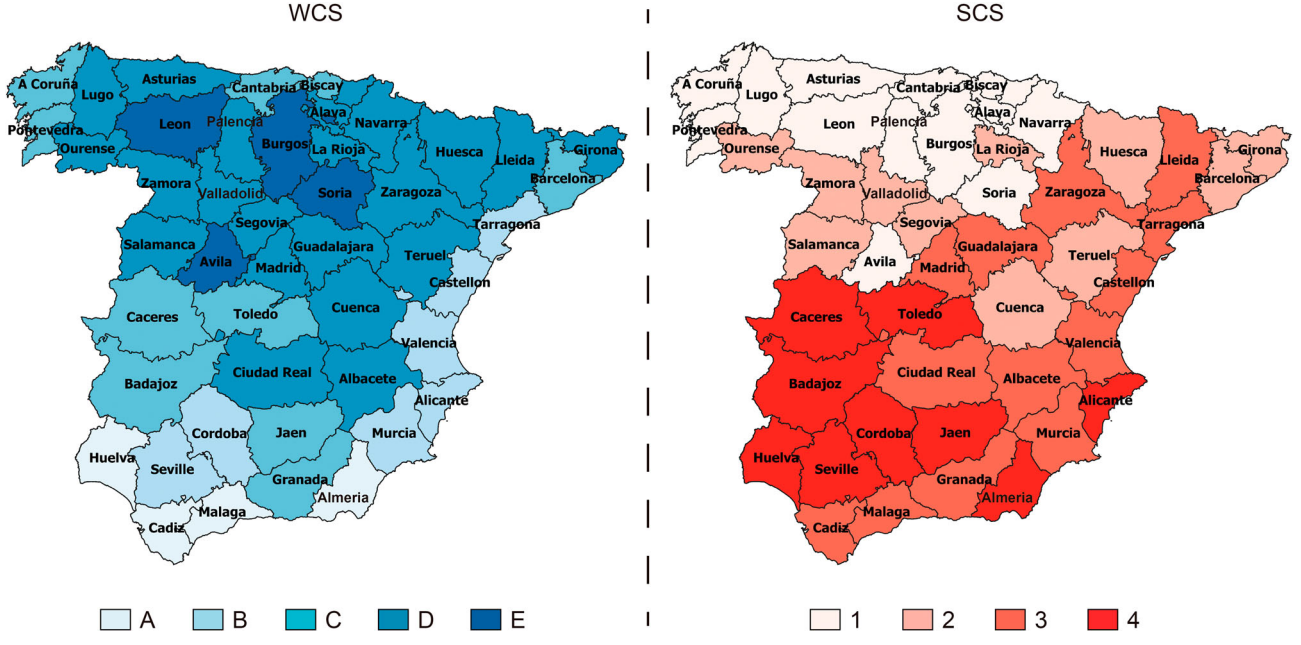

Figure 2. Climate severity of winter and summer in the provinces of Spain.

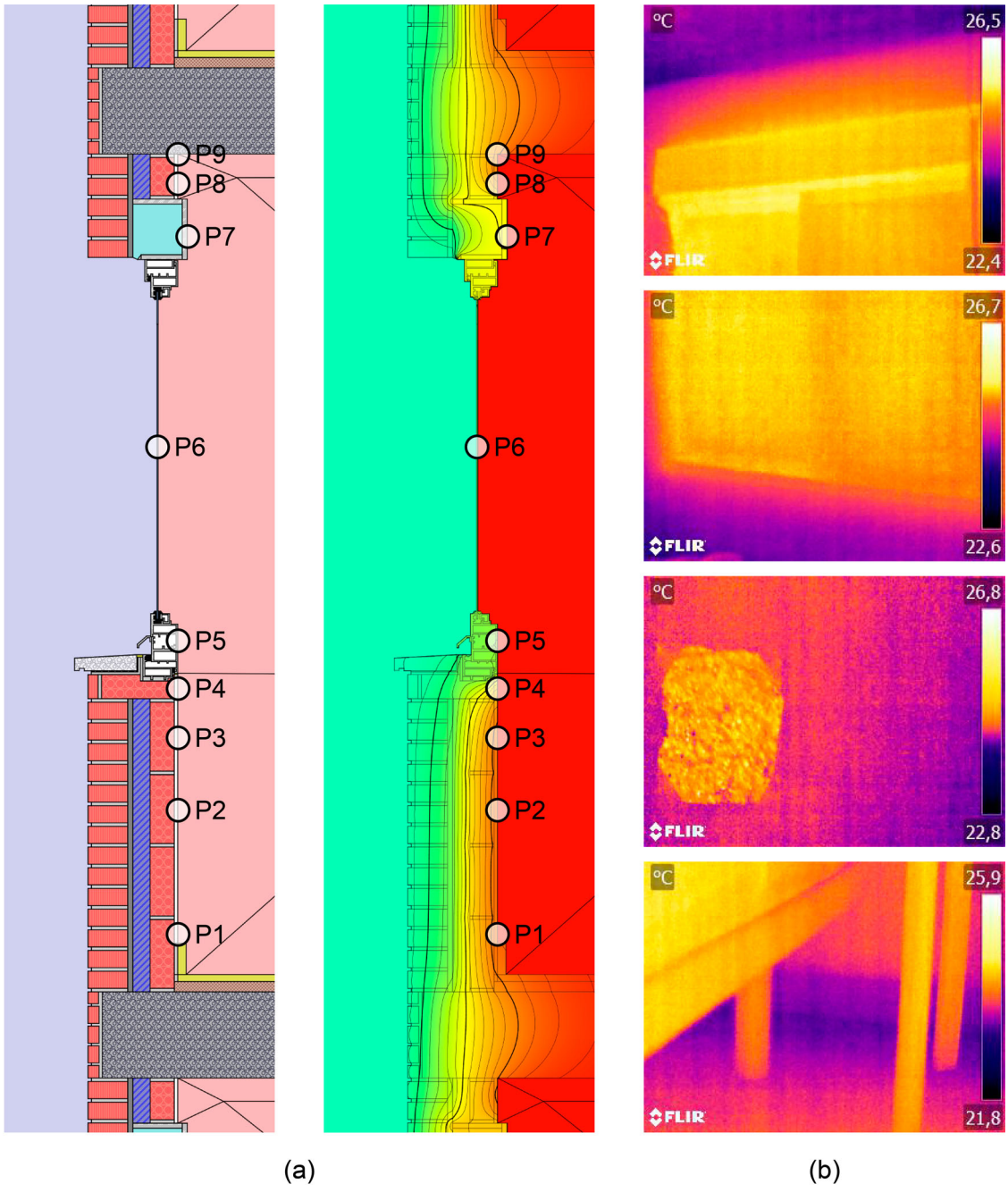

Figure 3. Simulation using HTflux: (a) simulation model using HTflux, and (b) thermograms carried out in the façade.

Simulation models

Surface temperatures were modelled by using the HTflux software, a two-dimensional transient calculation software according to ISO 10211. In total, 9 different points were analysed in the façade (see Figure 3(a)): (i) P1, junction of the wall with the inferior slab; (ii) P2, wall without any influence of thermal bridge; (iii) P3, the wall near to the thermal bridge of the window; (iv) P4, junction of the wall with the window; (v) P5, aluminium window frame; (vi) P6, glass of window; (vii) P7, aluminium frame of blind box; (viii) P8, junction of the wall with the blind box; and (ix) P9, junction of the wall with the superior slab. For such points, surface condensation risks were analysed (see Table 3). Layers, thickness, and properties of the materials were determined using reliable technical documentation. Table 4 indicates the configurations of

Table 3. The surface condensation risks analysed on each point.

Risk	Points
Corrosion of metal elements	P5 and P7
Mould growth	P1, P2, P3, P4, P8 and P9
Surface condensation	All

Table 4. Layer, thickness, and thermophysical properties of the building envelope.

	Layers				
Component	**Type**	s[mm]	λ[W/m · K)/W]	R[(m^2 · K)/W]	U[W/(m^2 · K)]
Wall	Cement mortar	10	1.000	–	1.35
	Hollow brick	70	0.375	–	
	Air gap	50	–	0.18	
	Cement mortar	15	1.300	–	
	Brick facing	115	1.042	–	
Window	Aluminium frame	10	–	0.17	5.89
	Simple glazing	3	0.900	–	
Floor	Terrazzo paving	20	1.800	–	1.76
	Sand	30	2.000	–	
	Floor slab	250	0.893	–	

the envelope elements. The values of internal and external surface resistance from ISO 13788 were used for each type of element. As can be seen, the façade of the case study corresponds to a common typology of multi-leaf walls with brick layers. Such façade typology is found in other countries, such as Italy (Corgnati, Fabrizio, Filippi, & Monetti, 2013), Belgium (Singh, Mahapatra, & Teller, 2013), and United Kingdom (Baker, 2011), so the results can be extrapolated to other regions.

The model was validated by comparing actual and simulated values. To do this, the façade was monitored (see Figure 3(b)). Thermograms were made with an infrared camera (FLIR E60bx), with a measurement range from −10 to 105°C, FOV of 25° × 19°, and IFOV of 1.36 mrad. Thermal sensitivity was lower than 0.05° C at 30°C, and the spectral range went from 7.5 to 13 µm. Thermograms were performed during sunset due to the availability of access to the dwelling of the user. In addition, aspects were considered as follows: (i) during 24 h before performing the thermogram, the external temperature was not greater than ±10°C with respect to the external temperature at the moment of performing the thermogram; and (ii) during performing the thermogram, the external temperature was not greater than ±5°C and the internal temperature was not greater than ±2°C with respect to the values of such variables at the moment of starting the performance of thermograms. Air temperature was measured with thermocouples type K. The measurement range of thermocouples went from −20 to 70°C, with a resolution of 0.1°C and an accuracy of ±0.2%. To assess the degree of adjustment, the Mean Bias Error (MBE) was analysed (Equation (7)). The limit value of 10% included in ASHRAE Guideline 14–2014 (ANSI/ASHRAE) was used (American National Standards Institute/American Society of Heating Refrigerating and Air-Conditioning Engineers (ANSI/ASHRAE), 2014). The MBE obtained in the monitorings of the 9 points was lower than 10%.

$$\mathrm{MBE} = \frac{\sum_{i=1}^{n} (y_i - x_i)}{n} \cdot 100 \quad [\%], \tag{7}$$

where n is the number of measures, y_i is the actual value, x_i is the simulated value, and $\bar{y}$ is the mean of actual values.

Internal environmental parameters (operative temperature and relative humidity) were obtained by means of a simulation with DesignBuilder. The validation of the model used in the building was already included in a previous study (Sánchez-García, Rubio-Bellido, Pulido-Arcas, Guevara-García, & Canivell, 2018).

Schedule values of heating and cooling setpoint temperatures as well as usage profiles were defined according to CTE (The Government of Spain, 2013). Table 5 indicates the schedule values associated with the setpoint temperatures. Simulations were performed with and without a ventilation system to see the improvement generated by the performance in the dwelling (incorporating a ventilation system) in the current state (without a ventilation system). The ventilation system had an air change rate of 0.63.

Estimation using ANNs

ANNs are one of the computational paradigms providing best features when facing statistical problems (Farshad, Garber, & Lorde, 2000), as nonlinear

Table 5. Setpoint temperatures of the residential profile of the CTE.

	Setpoint temperature [°C]								
	January – May			June – September			October – December		
Limit	**24–7**	**8–15**	**16–23**	**24–7**	**8–15**	**16–23**	**24–7**	**8–15**	**16–23**
Upper limit	–	–	–	27	–	25	27	–	25
Lower limit	17	20	20	–	–	–	17	20	20

relationships can be established among data (Bienvenido-Huertas, Rubio-Bellido, Pérez-Ordóñez, & Martínez-Abella, 2019). To automate the process of obtaining results of this research in new case studies, the simulation process was automated.

In this study, the multilayer perceptron (MLP) was used as an architecture of ANN. This architecture is made up of three or more layers: (i) an input layer, which obtains the information from the input variables; (ii) one or several intermediate layers, which extract the information required; and (iii) an output layer, which estimates the output value of the model. The output value of the last layer corresponds to the sum of the output values of the weighted intermediate layers, which are obtained through the weighted values of the input layer (see Equation (8)). Hours of risk of corrosion (h_{corr}), humidity (h_{mould}), and surface condensation (h_{dew}) were analysed. However, ISO 13788 uses monthly data. Thus, the possibility of estimating hours with risk was analysed by using both monthly temperature data (T_{in}; T_{out}; $T_{s,in}$) and internal relative humidity data (RH_{in}). Likewise, the estimation of the temperature factor at the internal surface for the year 2050 ($f_{R_{si}}2050$) with current data was also analysed. Thus, four MLPs were analysed (see Figure 4).

$$z = \sigma\left(\sum_{j=1}^{M} w_{kj}^{(2)}\sigma\left(\sum_{i=0}^{d} w_{ji}^{(1)}x_i\right) + w_{k0}^{(2)}y_0\right), \tag{8}$$

where z is the value of the output layer, σ is the activation function, x_i are the input layer values, y_0 and $w_{k0}^{(2)}$ are the input value and the weight of the bias neuron of the hidden layer, respectively, $w_{ji}^{(1)}$ are the weights of the hidden layer, and $w_{kj}^{(2)}$ are the weights of the output layer.

MLPs were trained by using the Broyden–Fletcher–Goldfarb–Shanno (BFGS) algorithm (Fletcher, 1980). Trainings were performed by means of 10-fold cross validation, and a sigmoidal activation function was used (see Equation (9)). Architectures of one layer in the hidden layer were considered because they usually have a better behaviour than more complex architectures (Kumar, Aggarwal, & Sharma, 2013). The MLPs were optimized by determining the most adequate number of nodes for the hidden layer. To generate datasets, the data obtained from the simulations run in each climate zone were used. Individual datasets were used for each climate zone, and a combined one for all climate zones. Such datasets were divided into two subsets: a training (with 75% of instances) and a testing subset (with 25% of instances). They were randomly generated. Moreover, a learning rate of 0.3 and a momentum of 0.2 were used as fixed parameters of the MLPs.

$$\sigma = \frac{1}{1+e^{-x}}, \tag{9}$$

where x is the weighted sum of inputs in the node.

The statistical parameters, which are quality indicators of the MLPs, were the correlation coefficient (R^2) and the mean absolute error (MAE):

$$R^2 = 1 - \frac{\sum_{i=1}^{n}(x_i - y_i)^2}{\sum_{i=1}^{n}(x_i - \bar{x}_i)^2}, \tag{10}$$

$$\mathrm{MAE} = \frac{\sum_{i=1}^{n}|y_i - x_i|}{n}. \tag{11}$$

Results and discussion

Surface condensation risks in climate zones in the current scenario

First, values of surface temperatures of the different points were simulated. Figure 5 shows an example of the values simulated in P2 and P6 in the area A3, and Figure 6 reflects the existing correlation between the surface temperature and the boundary conditions in area A3. As can be seen in Figure 6, the internal surface temperature presented a high correlation with the internal air temperature. The values of R^2 for the various points in each area were higher than 0.70, and the points with the greatest correlation were those of the wall (P1, P2, P3, and P9). The points with the lowest R^2 were those of the window (P5 and P6). However, the correlation of the internal surface temperature with the external air temperature presented a different behaviour. On the

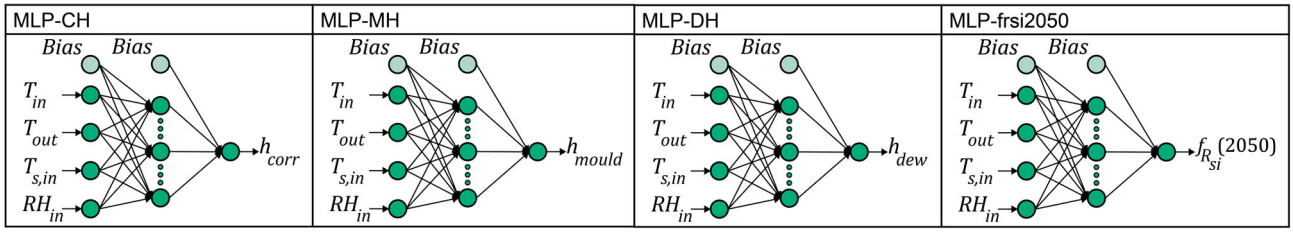

Figure 4. Scheme of the architectures of the MLPs.

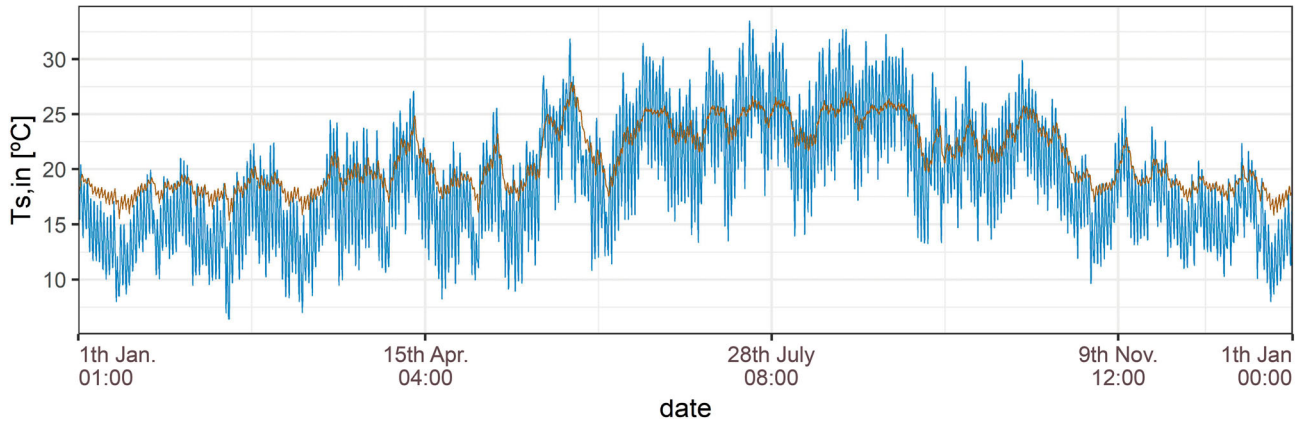

Figure 5. Internal surface temperature of P2 (brown line) and P6 (blue line) in the area A3.

one hand, the correlation was higher in the elements of greater thermal transmittance (*i.e.* with a low thermal resistance), such as the window frame (P5) and the glass (P6), with a R^2 higher than 0.95. Also, the points that presented a bidimensional flux due to the finishing work of the window also had a correlation greater than the external temperature. This anticipated that such points were the most unfavourable points of the façade for the surface condensation risk. On the other hand, the correlation was lower in the elements with greater thermal resistance. This explains why the fluctuations of the surface temperature of such points were greater than that of other points, such as P2 (Figure 5 shows that the fluctuation of P6 is greater than P2).

After analysing the existing relationship between the boundary conditions and the surface temperature of points, the number of hours with surface condensation risk was obtained. As previously mentioned, the risks of corrosion of metal elements, mould growth, and surface condensation were analysed. For this purpose, values of critical relative humidity set by ISO 13788 were used. Figure 7 shows the number of hours with the risks associated with surface condensation. As can be seen, the behaviour obtained in the different areas was not the same. Regarding the hours with risk of mould growth, the areas with the greatest risk were those with a lower WCS (areas A and B), in which the number of hours presented a percentage increase between 6.52% and 165% with respect to the maximum number of hours reached by the other areas (areas C, D, and E). This aspect is in accordance with Becker (1993), who reflected the greatest risk of mould in moderate climates. In addition, the area A4 was the one which obtained the greatest number of mould growth, with a mean increase of 168 h with respect to the following area with a larger number of hours (B3). Likewise, the point with the greatest risk of mould growth is the junction of the wall with the aluminium window frame (P4). The number of hours in such point was always greater than 60% with respect to the following point with the greatest mould growth (P8). In addition, the thermal bridge of the slab front did not generate a huge increase of the number of hours. In this sense, the increase presented by the number of hours related to the risk of mould growth with respect to the wall without any influence of the thermal bridge was lower than 31.25% and 54.05% for the thermal bridge of the floor and ceiling, respectively. This highlighted several important aspects because the effect of the thermal bridge of the slab in the surface condensation risk was not significant in the case of old buildings, mainly due to the low coupling coefficient of the joint (the thermal resistances of the two elements joint were similar, unlike walls with good insulation). Also, the effect caused by the window in the opaque area of the façade was quite significant because they were the main areas where mould appeared.

Concerning the risks of corrosion of metal elements in both points of woodwork, the number of annual hours with risk of corrosion was higher than 4,500. Furthermore, the behaviour among climate zones was similar to that of mould growth. In this regard, the areas with a lower WCS were those obtaining a larger number of hours with risk of corrosion, and the area A4 obtained the greatest number of hours. As can be seen in Figure 7(b), areas A3, A4, and B3 obtained an increase greater than 1.34% and 1.14% for P5 and P7, respectively, with respect to the other areas. Only one area with a lower WCS obtained less hours than the remaining areas with a greater WCS. Area B4 obtained values lower than in C2, C4, D2, and E1 in P5, and areas D3 and E1 in P7. From the two points analysed, Figure 7(b) shows that the point of the window frame (P5) obtained a greater risk of corrosion than the point of the frame of the blind box (P7), with an increase between 0.45 and

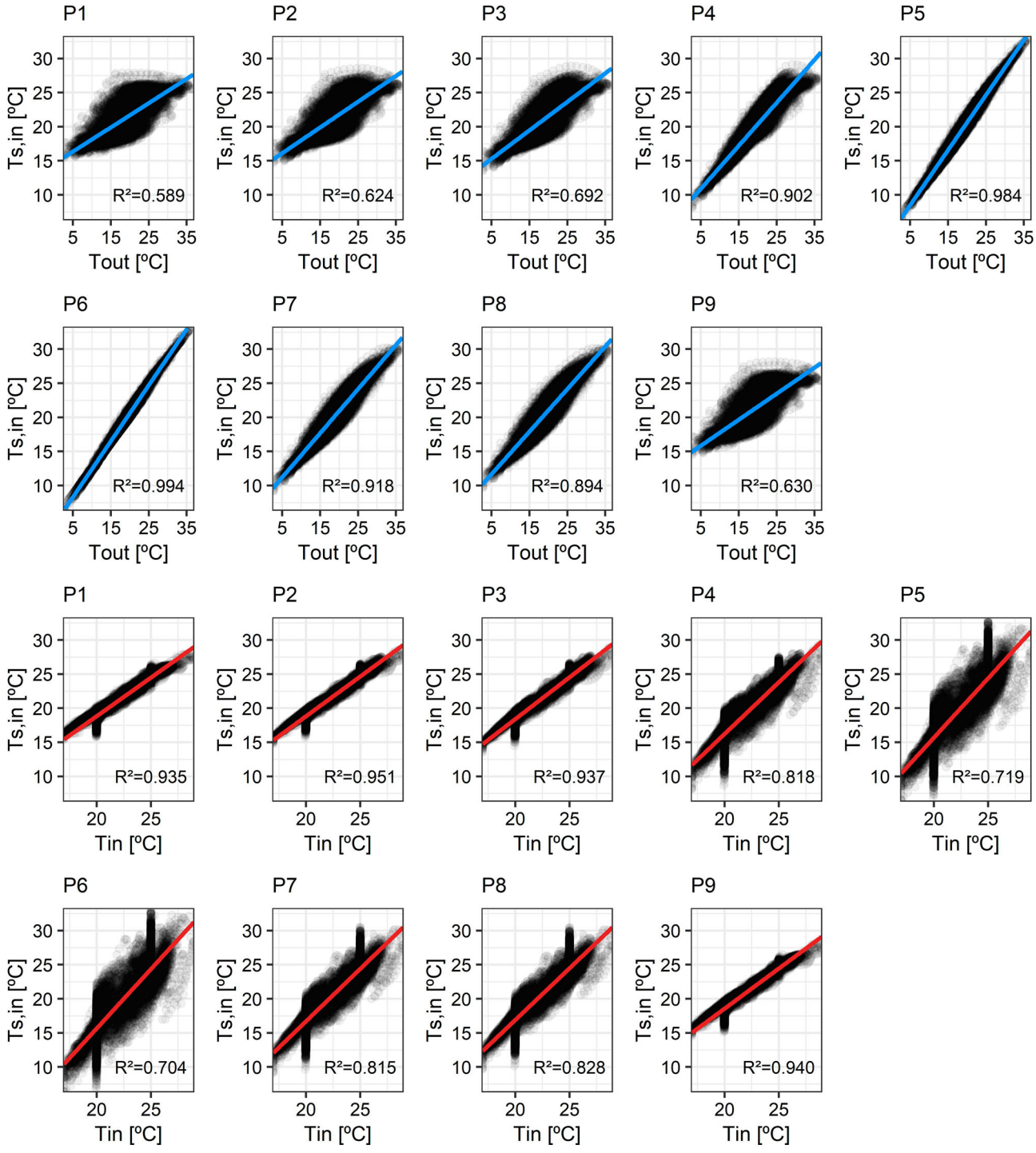

Figure 6. Scatter plot of internal surface temperature and internal and external air temperatures in the area A3.

23.12% in the percentage of hours. This is because the thermal transmittance of the window frame is greater than that of the frame of the blind box (this last one has the external layer of brick). The metal points of the façade are therefore very likely to present risks of corrosion throughout its useful life. This aspect would imply users to replace them throughout the years due to the damages presented.

Regarding hours of surface condensation, Figure 7(c) indicates the values obtained by each point of the façade. The point with the greatest surface condensation risk is the glass of the window (P6), followed by the window frame (P5). This result is quite important because condensed water can be extended to other areas of the façade if the drying of these elements is not produced, thereby causing degradation. This

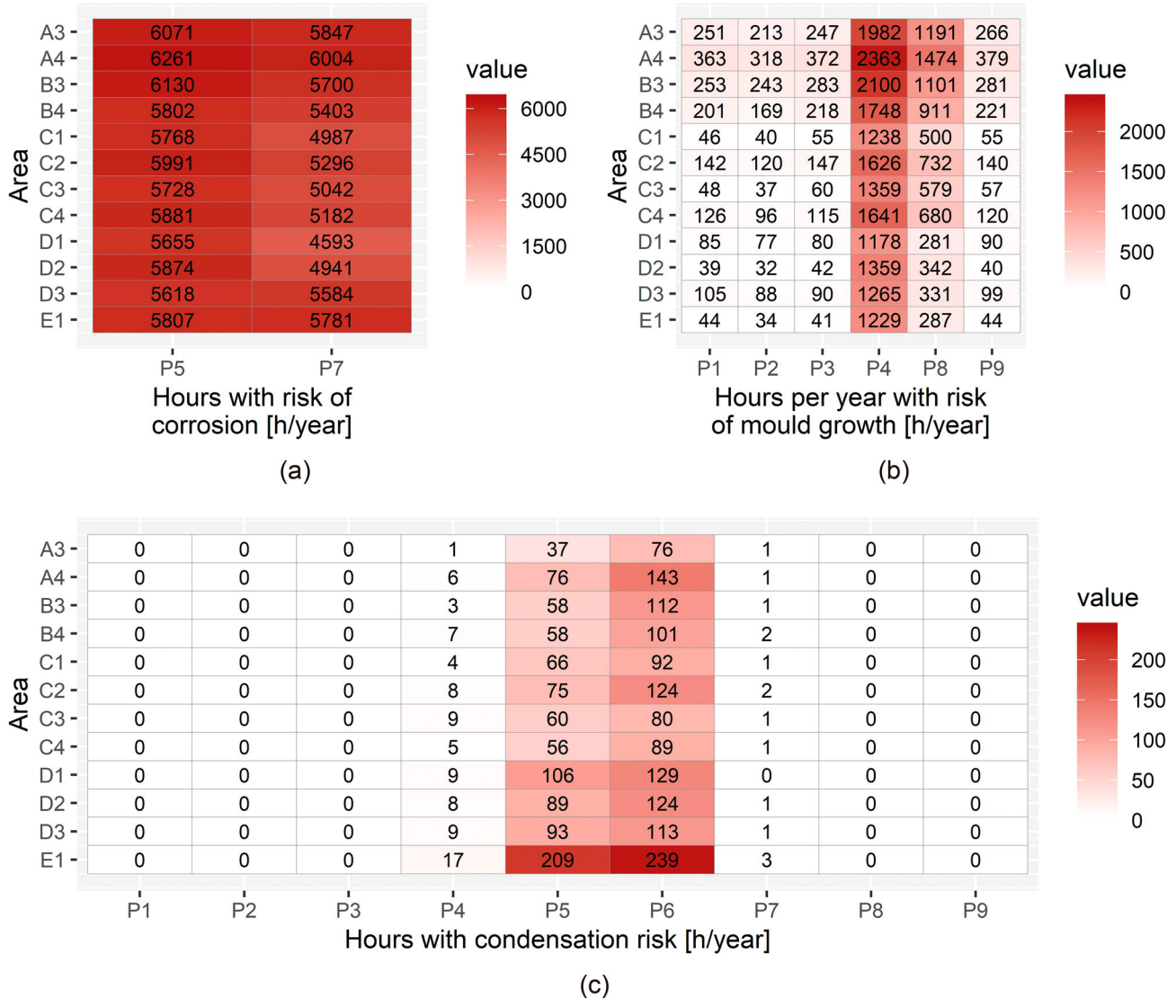

Figure 7. Surface condensation risk in the current scenario: (a) hours per year with risk of mould growth, (b) hours per year with risk of corrosion, and (c) hours per year with surface condensation risk.

showed the common problems of buildings with windows, in which bad ventilation and bad thermal properties of the window were a main point of condensations (Emenius et al., 2004; Hägerhed-Engman, Bornehag, & Sundell, 2009). Also, the points corresponded to the wall of façade (P1, P2, P3, P8, and P9) did not present surface condensations. Only the point of the thermal bridge between the window and the wall (P4) presented hours with surface condensation oscillating between 1 and 17. With respect to the existing difference among the climate zones, the behaviour obtained for hours with risk of mould growth and corrosion was not obtained for hours of condensation. In this way, areas with a greater WCS obtained higher values than areas with a lower WCS, with a mean increase in each area between 27.57% and 84.17%. Despite having less hours with risk of mould growth, values of surface relative humidity were higher than in the areas with a lower WCS, thereby causing the value of critical relative humidity for surface condensation to be exceeded (see Figure 8). Thus, the area E1 was the one which obtained the greatest number of hours with surface condensation risk, with an increase higher than 85.27% with respect to the following area with greater number of hours (D1).

The various climate zones had therefore favourable conditions for the appearance of condensation problems in the building typology analysed. The typical characteristics of each zone implied different behaviours in each type of risk, but a high appearance of such problems was detected in all of them, thereby causing two aspects: (i) the possibility of a low IAQ, with the risk of

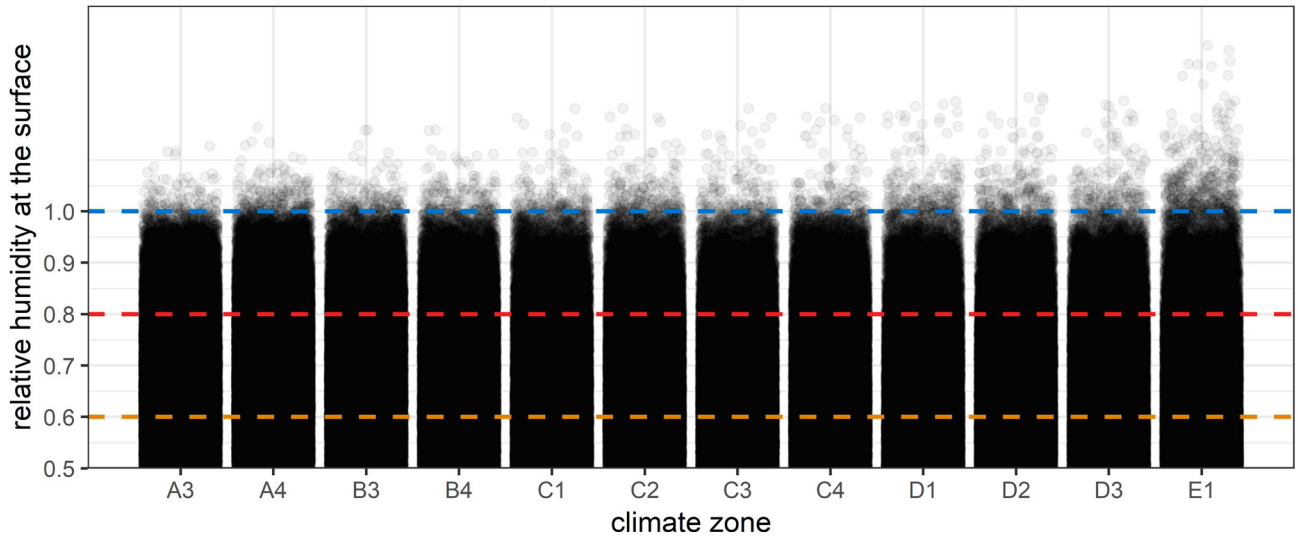

Figure 8. Jitter plot of the relative humidity at the surface of the façade for each climate zone. Values of critical relative humidity of condensation, mould growth, and corrosion are represented by blue, red, and orange lines, respectively. Points with values higher than 1 are related to surface condensation.

respiratory health for users; and (ii) possible damages in the elements of the façade of such buildings.

Influence of climate change in 2050

The scenario of A2 greenhouse gas emissions for the year 2050 changed the number of hours with risk which were obtained in the current scenario. The number of hours with risk of corrosion, mould, and condensation had different variations, increasing or reducing the number depending on the type of risk. This was because of the variations presented by the limit $f_{R_{si}}$ obtained at each instant. Although, at first, the effect of climate change causes a reduction of the external relative humidity and an increase of the external air temperature, the thermal gradient between the internal and external temperature presented a mean increase of 2.44°C in the coldest months. This implied that $f_{R_{si}}$ of mould and surface condensation increased with respect to the current scenario, whereas the $f_{R_{si}}$ of corrosion decreased or increased depending on the environmental conditions (see Figure 9). Such variations caused the number of hours with risk of mould and condensation to be increased in those points with a greater correlation with the external air temperature (see Figure 5). As the limit value is greater, a larger number of hours are below such value.

Tables 6–8 represent the variations in the number of hours with risk in 2050. Regarding the hours of corrosion, given that the limit $f_{R_{si}}$ for corrosion presented reductions, the number of hours with risk of corrosion was lower. Table 6 shows that the oscillation of the percentage of reduction for both points was between 42.8% and 57.63%.

The risk of mould growth in 2050 had two different behaviours (see Table 7): (i) the points with the greatest thermal resistance (P1, P2, P3, and P9) presented percentage reductions between 5.26% and 94.12% for all the areas; and (ii) the points influenced by the window (P4 and P8) presented a percentage increase of 3.17% and 37.01%, respectively. Only in the area E1, a reduction of the number of hours of P4 was achieved. In this way, the surface condensation risk had a similar behaviour (see Table 8): (i) the points with the lowest thermal resistance presented an increase of the number of hours; and (ii) the points with the greatest thermal resistance did not have hours with condensation. Also, there was a decreasing tendency in the number of hours in the areas with a greater WCS. This behaviour was different to that obtained in the current scenario because the thermal gradient obtained in the areas with a lower WCS was greater than that obtained in areas with a greater WCS (heating setpoint temperatures were not exceeded in areas with a greater WCS, whereas these temperatures were exceeded in areas with a lower WCS, so the thermal gradient increased).

It was found that the predicted environmental conditions due to climate change will significantly influence the decrease of surface condensation cases. The increase of average temperatures and the decrease of the relative moisture reduces the conditions which contribute to the surface condensation risk. This aspect was not detected in zones with a low thermal resistance. The improvement of the thermal resistance in such points would reduce the surface condensation risk in the next years. It is worth highlighted that it does not mean that environmental conditions are improved by climate

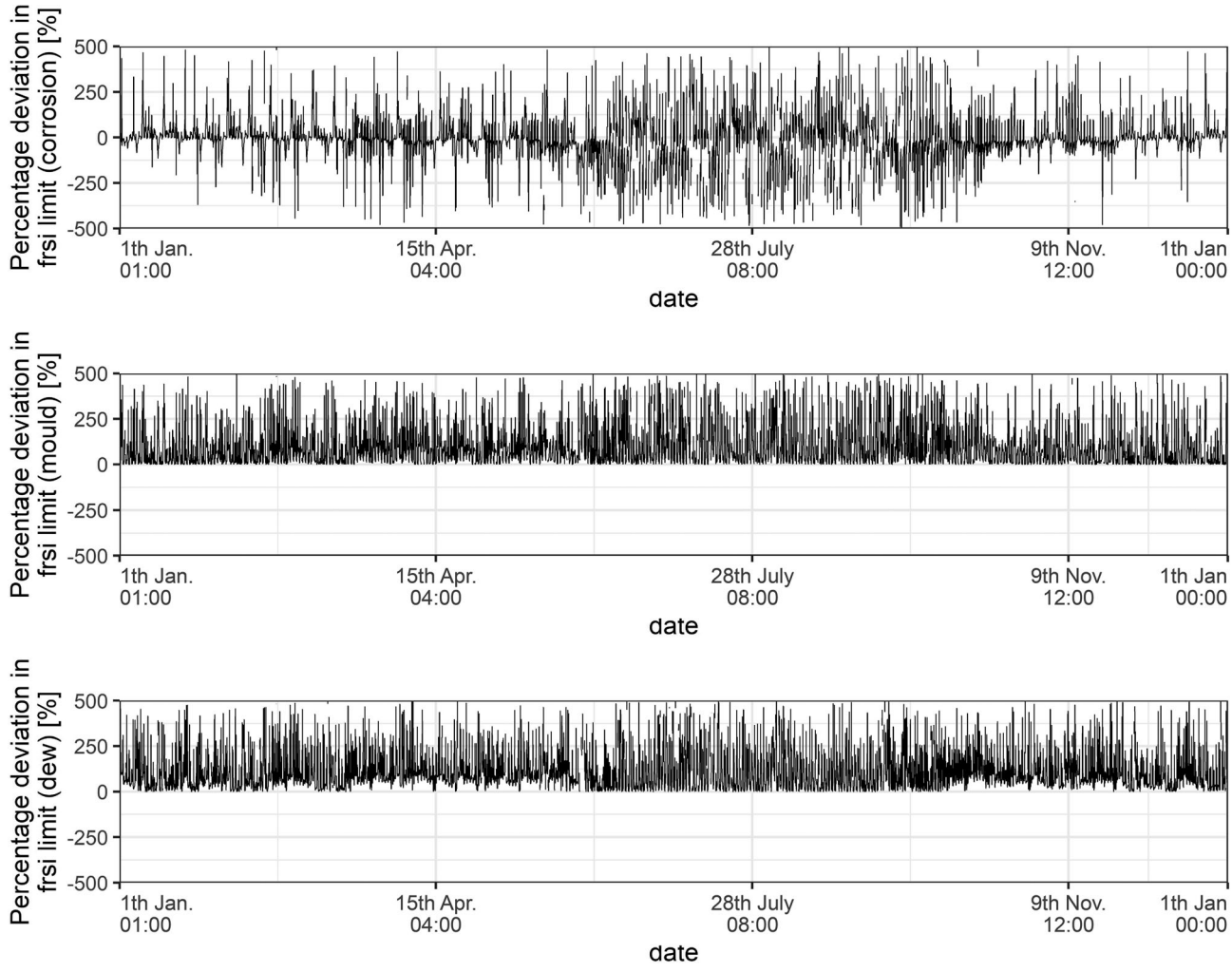

Figure 9. Deviation percentage of the limit $f_{R_{si}}$ of the scenario 2050 with respect to the current scenario in the area A3.

change, but a tendency of decrease is detected in the cases of surface condensation.

Incorporating a ventilation system

The implementation of a ventilation system allowed the surface condensation risk to be reduced in all climate zones. In this sense, the number of hours with risk of corrosion in P5 and P7 presented reductions greater than 47% and 19% in the current scenario and 2050, respectively (see Figure 10(a)). Likewise, the number of hours with risk of mould formation almost disappeared (see Figure 10(b)). Only some points in the current scenario presented hours with such risk, but the reduced number (lower than 20) allowed the effectiveness of having these systems to be guaranteed in order to remove the surface condensation risk in the existing buildings. For the year 2050, the risk of mould formation disappeared. Therefore, hours with surface condensation were not obtained in 2050. For the current scenario, although hours with mould formation were obtained, the relative humidity at the surface was lower than 100%, so hours with surface condensation were not obtained. Thus, these results corroborate the effectiveness of using a ventilation system as a way to remove surface condensation risks in most of the building stock in Spain. Also, the results obtained by using the ventilation system allowed better reduction percentages to be obtained in the condensation risk than those analysed in other studies, such as the study by Liu et al. (2004) in which a decrease of 26% was obtained. It is therefore an effective measure to solve condensation problems in the existing buildings. Also, it allows the impact caused by the user' behaviour to be reduced.

Estimation using MLPs

As mentioned in Section 2.6, three MLPs were suggested due to the huge amount of time required to carry out the schedule analysis of the surface condensation risk. Each MLP determined the number of hours for each limit value of surface humidity: corrosion (MLP-CH), mould (MLP-MH), and surface condensation (MLP-DH).

Table 6. Deviation percentage of hours per year with risk of corrosion in 2050.

	Deviation percentage [%]	
Areas	**P5**	**P7**
A3	−53.29	−51.26
A4	−53.59	−51.48
B3	−54.39	−50.54
B4	−53.84	−49.99
C1	−56.02	−47.00
C2	−55.90	−48.64
C3	−57.63	−50.04
C4	−57.39	−50.60
D1	−55.15	−42.80
D2	−55.99	−46.25
D3	−56.76	−55.39
E1	−55.42	−53.50

Table 7. Deviation percentage of hours per year with risk of mould growth in 2050.

	Deviation percentage [%]					
Area	**P1**	**P2**	**P3**	**P4**	**P8**	**P9**
A3	−38.65	−50.23	−39.68	18.92	28.46	−34.96
A4	−40.50	−55.97	−47.04	5.63	18.11	−39.05
B3	−64.82	−74.90	−60.78	8.95	22.71	−62.63
B4	−57.21	−68.05	−59.17	21.85	30.30	−54.75
C1	−19.57	−20.00	−10.91	26.58	21.00	−5.45
C2	−45.07	−49.17	−27.89	8.18	6.01	−29.29
C3	−6.25	−16.22	−33.33	18.18	20.38	−5.26
C4	−65.87	−75.00	−66.09	3.17	9.12	−60.83
D1	−51.76	−50.65	−35.00	14.86	37.01	−41.11
D2	−71.79	−75.00	−73.81	8.68	27.49	−72.50
D3	−66.67	−67.05	−60.00	4.58	7.55	−61.62
E1	−84.09	−94.12	−82.93	−1.14	4.53	−81.82

Table 8. Variation in the number of hours per year with surface condensation risk in 2050.

	Variations of the hours with condensation risk [h/year]								
Areas	**P1**	**P2**	**P3**	**P4**	**P5**	**P6**	**P7**	**P8**	**P9**
A3	0	0	0	7	409	550	1	0	0
A4	0	0	0	12	493	638	1	0	0
B3	0	0	0	1	286	388	1	0	0
B4	0	0	0	−3	286	399	0	0	0
C1	0	0	0	2	200	308	0	0	0
C2	0	0	0	−4	37	62	−1	0	0
C3	0	0	0	−5	79	346	0	0	0
C4	0	0	0	−2	80	139	0	0	0
D1	0	0	0	−3	16	59	3	0	0
D2	0	0	0	−2	44	85	2	0	0
D3	0	0	0	−4	10	57	1	0	0
E1	0	0	0	−8	−28	−19	−1	0	0

Likewise, the degree of adjustment presented by the MLP among individual models for each climate zone was analysed, together with a model covering all areas. Figure 11 represents the values obtained by the statistical parameters and the optimal number of nodes of the hidden layer (H). All MLPs presented an adequate architecture, with a number of nodes between 4 and 8. The R^2 obtained in the training of all MLPs was greater than 90%. Furthermore, the statistical parameters of error in the training presented acceptable values. MAE obtained values between 9.91 and 29.21. Regarding the testing, values similar to the training were obtained. The correlation coefficient obtained by the models was greater than 97%. Thus, there was a low dispersion between the actual values and those estimated by the models (see Figure 11). The parameters of error presented values similar to those obtained in the training. With respect to the best adjustment between the specific models of each area and the models which are useful for all areas, there were great differences among the statistical parameters. In some MLPs, such as MLP-CH A3 or MLP-MH C4, the R^2 obtained was slightly higher. Moreover, in other specific models, the degree of adjustment was lower than the generic model. Thus, the effect of using individual models in each area did not mean an improvement in the degree of adjustment of the model. Therefore, the use of a model for all areas determined, with a degree of acceptable accuracy, the number of hours with the different risks related to surface condensation.

In addition, a model determining the $f_{R_{si}}$ in 2050 with data from current scenario was suggested. Like for the MLPs of hours, the possibility of developing both individual models for each area and a generic model for all was analysed. Figure 12 indicates the values obtained in the training and testing. The architecture of the hidden layer was similar to that of the previous MLPs, since the number of nodes of the hidden layer was between 6 and 8. Regarding the degree of adjustment in the training phase, R^2 was between 86% and 94%, and MAE was in all cases 0.10 or lower. Thus, all models obtained an acceptable degree of adjustment. Concerning the testing, the values obtained were like those from the training phase. The estimated values presented an adequate degree of adjustment with respect to the actual values of the subsets of the testing (see Figure 12). Regarding which model obtained the best performance, the same tendency as in the schedule MLPs can be seen. In this sense, the specific models of each area obtained R^2 presenting variations between −4.19% and 4.75% with respect to that obtained by the generic model. Such variations mean again that there is not a significant difference between the specific models of each area and the generic model. As a result, there is

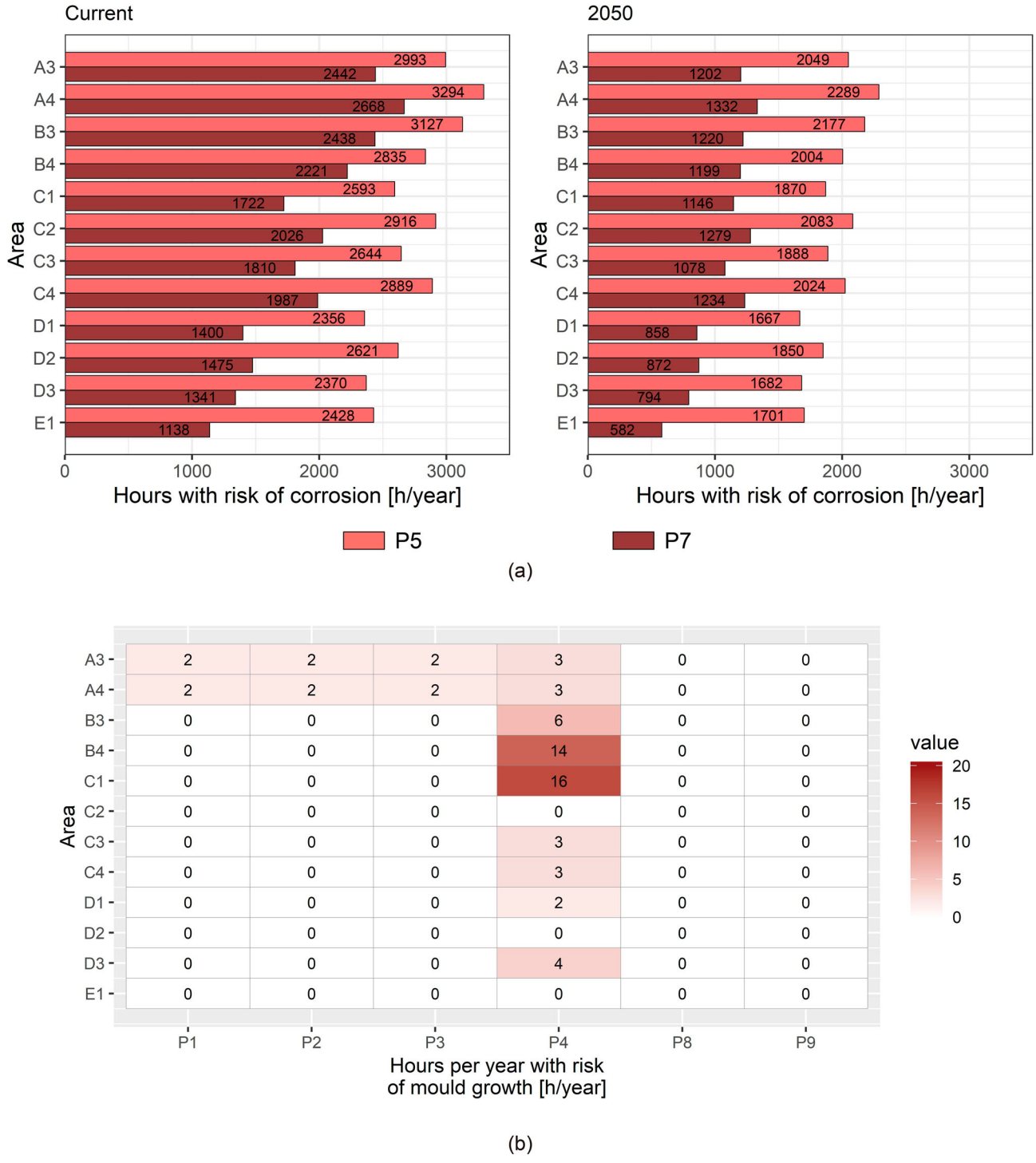

Figure 10. The effect of implementing a ventilation system: (a) hours with risk of corrosion in case of incorporating a ventilation system (current scenario and 2050), and (b) hours per year with risk of mould growth in case of incorporating a ventilation system (current scenario).

coherence among the ANNs developed: the use of specific models for each climate zone does not obtain a greater accuracy in the estimated value. By using such prediction models, accurate analyses can be performed with monthly mean values, thus constituting a useful tool for engineers and architects.

Conclusions

The results determined that the areas with a soft winter presented a higher risk of mould formation, whereas areas with a severe winter presented a higher surface condensation risk. Likewise, the area with the greatest

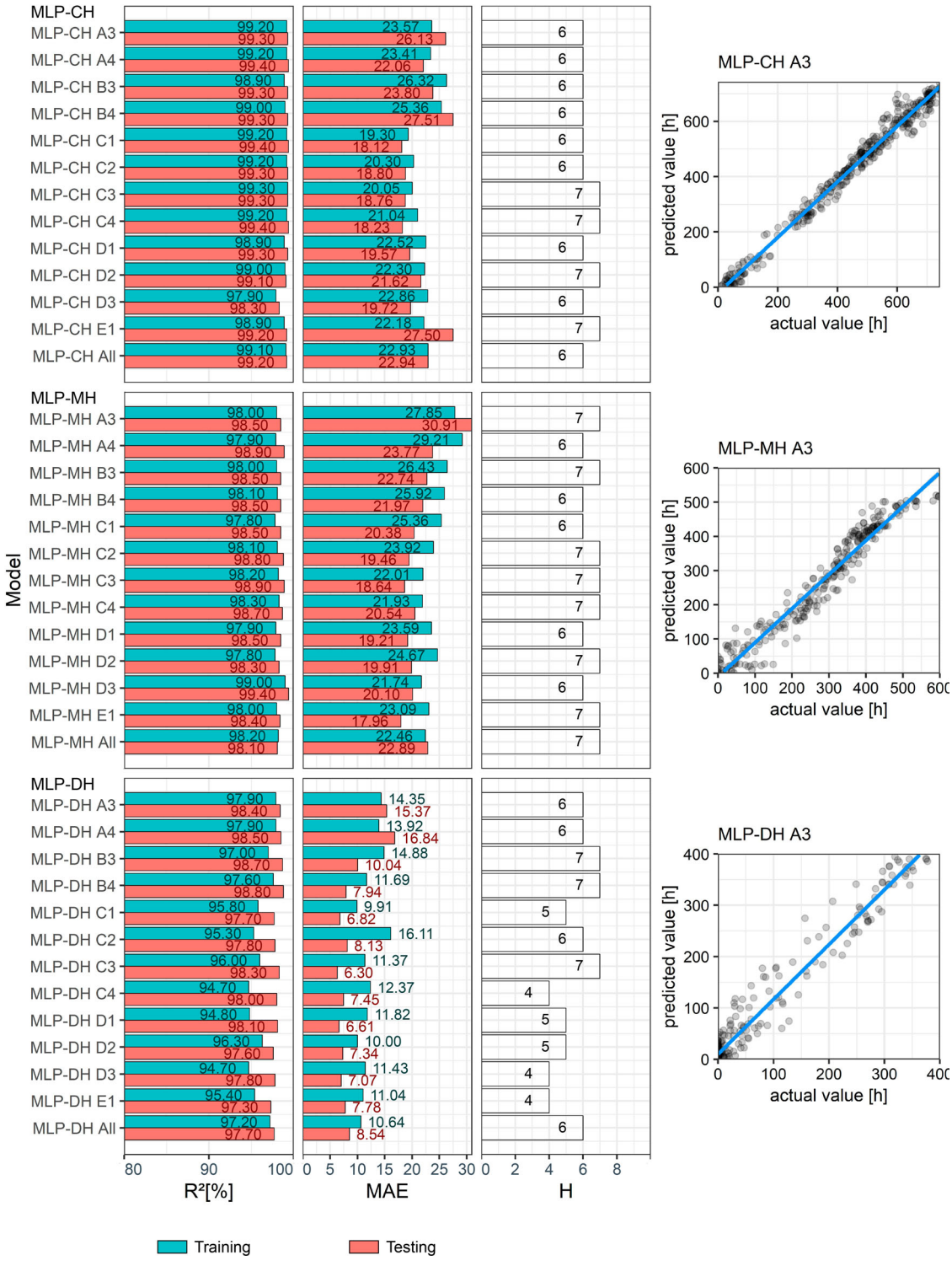

Figure 11. Behaviour of MLP-CH, MLP-MH, and MLP-DH models, and correlation between the actual and the estimated value in the testing carried out for MLP-CH A3, MLP-MH A3, and MLP-DH A3.

risk of mould formation was the area of the wall near to the window, whereas the glass was the point with the largest number of hours with surface condensation. The results reflect the combination of two aspects affecting users in relation to the surface condensation in the building typology analysed. On the one hand, the number of cases with surface condensation risk highlights the possibility that users have a low air quality inside the rooms, thus implying the appearance of allergy symptoms and respiratory problems. On the

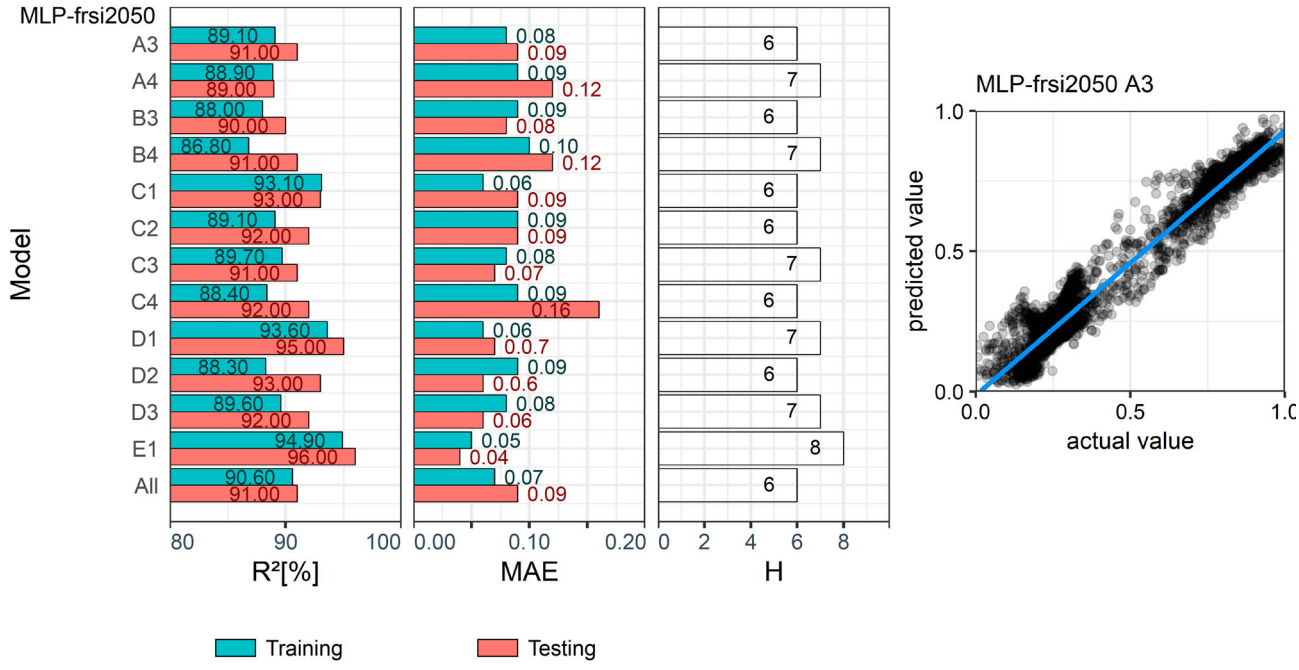

Figure 12. Behaviour of MLP-frsi2050 models and correlation between the actual and the estimated value in the testing carried out for MLP-frsi2050 A3.

other hand, the high risk of corrosion of the metal elements of the façades can contribute to the appearance of damages which would reduce the useful life of such elements. In this way, the high influence of windows on surface condensations stresses the need of improving such elements in order to obtain reductions in condensation cases.

The 2050 scenario generated an increase in the limit $f_{R_{si}}$, leading in turn to an increase in the number of hours with risk of mould formation and condensation in points with less thermal resistance. However, the environmental conditions predicted for such scenarios significantly reduced the percentage of hours with risks (of different types) in most of the points in the façade. This does not mean that climate conditions are better in future scenarios, but a decrease in condensation cases. The use of windows with better thermal characteristics allowing greater surface temperatures in such points to be kept would therefore reduce the surface condensation risk in the future.

What is previously indicated corresponds to cases in which the ventilation is deficient. This means that, apart from the condensation risk, the air quality could be deficient in the room. The use of ventilation systems would allow several advantages to be obtained. Besides the improvement of the air quality due to its renovation, the surface condensation risk both in the current scenario and 2050 can be removed by using ventilation systems. The results showed that the use of a ventilation system, according to the Spanish Building Technical Code, reduced such numbers of hours by 0. This could be achieved without the need of replacing the windows.

Moreover, multilayer perceptrons have been suggested to estimate hours with surface condensation risk, as well as to estimate such risk in 2050. The high correlation obtained in the training and testing phases, together with the low error obtained, guarantees the viability of using these prediction models. In addition, having individual and predicted models for each climate zone was not required (*i.e.* the use of prediction models allowing estimations to be performed in all climate zones has similar performances with respect to the typical models of each climate zone).

To conclude, the results can be useful to allow architects and engineers to propose improvements in buildings with degradation because of surface condensations. The international aspect of the results is found in the case study analysed (it is a typology of façade used in various countries, such as Italy, Belgium, and United Kingdom) and the climate zones analysed, which are in many countries, particularly in the Mediterranean area. Thanks to these prediction models, a greater knowledge of the surface condensation risk of the façade of buildings could be obtained. Future steps of this research will be focused on analysing the risk of external condensation.

Disclosure statement

No potential conflict of interest was reported by the authors.

ORCID

David Bienvenido-Huertas http://orcid.org/0000-0003-0716-8589
Carlos Rubio-Bellido http://orcid.org/0000-0001-6719-8793
Daniel Sánchez-García http://orcid.org/0000-0002-3080-0821
Juan Moyano http://orcid.org/0000-0002-2186-6159

References

American National Standards Institute/American Society of Heating Refrigerating and Air-Conditioning Engineers (ANSI/ASHRAE). (2014). *ASHRAE guideline 14-2014: Measurement of energy, demand, and water savings*. Atlanta, GA: ASHRAE.

Antonyová, A., Korjenic, A., Antony, P., Korjenic, S., Pavlušová, E., Pavluš, M., & Bednar, T. (2013). Hygrothermal properties of building envelopes: Reliability of the effectiveness of energy saving. *Energy and Buildings*, *57*, 187–192. doi:10.1016/j.enbuild.2012.11.013

Baker, P. (2011). *U-values and traditional buildings: In situ measurements and their comparisons to calculated values* (Historic Scotland Technical paper 10). Glasgow, UK: Technical Conservation Group.

Barreira, E., & de Freitas, V. P. (2013). Experimental study of the hygrothermal behaviour of external thermal insulation composite systems (ETICS). *Building and Environment*, *63*, 31–39. doi:10.1016/j.buildenv.2013.02.001

Becker, R. (1984). Condensation and mould growth in dwellings-parametric and field study. *Building and Environment*, *19*(4), 243–250. doi:10.1016/0360-1323(84)90005-2

Becker, R. (1993). Effects of heating patterns on internal surface temperatures and risk of condensation. *Building and Environment*, *28*(3), 333–345. doi:10.1016/0360-1323(93)90038-5

Becker, R., & Jaegermann, C. (1982). The influence of the permeability of materials and absorption on condensation in dwellings. *Building and Environment*, *17*(2), 125–134. doi:10.1016/0360-1323(82)90049-X

Bekö, G., Lund, T., Nors, F., Toftum, J., & Clausen, G. (2010). Ventilation rates in the bedrooms of 500 Danish children. *Building and Environment*, *45*(10), 2289–2295. doi:10.1016/j.buildenv.2010.04.014

Belcher, S., Hacker, J., & Powell, D. (2005). Constructing design weather data for future climates. *Building Services Engineering Research and Technology*, *26*(1), 49–61. doi:10.1191/0143624405bt112oa

Bellia, L., & Minichiello, F. (2003). A simple evaluator of building envelope moisture condensation according to an European Standard. *Building and Environment*, *38*(3), 457–468. doi:10.1016/S0360-1323(02)00060-4

Bienvenido-Huertas, D., Moyano, J., Rodríguez-Jiménez, C. E., & Marín, D. (2019). Applying an artificial neural network to assess thermal transmittance in walls by means of the thermometric method. *Applied Energy*, *233–234*(June 2018), 1–14. doi:10.1016/j.apenergy.2018.10.052

Bienvenido-Huertas, D., Rubio-Bellido, C., Pérez-Ordóñez, J., & Martínez-Abella, F. (2019). Estimating adaptive setpoint temperatures using weather stations. *Energies*, *12*(7), 1197. doi:10.3390/en12071197

Cho, W., Iwamoto, S., & Kato, S. (2016). Condensation risk due to variations in airtightness and thermal insulation of an office building in warm and wet climate. *Energies*, *9*(11), doi:10.3390/en9110875

Corgnati, S. P., Fabrizio, E., Filippi, M., & Monetti, V. (2013). Reference buildings for cost optimal analysis: Method of definition and application. *Applied Energy*, *102*, 983–993. doi:10.1016/j.apenergy.2012.06.001

Dallongeville, A., Le Cann, P., Zmirou-Navier, D., Chevrier, C., Costet, N., Annesi-Maesano, I., & Blanchard, O. (2015). Concentration and determinants of molds and allergens in indoor air and house dust of French dwellings. *Science of the Total Environment*, *536*, 964–972. doi:10.1016/j.scitotenv.2015.06.039

Dimitroulopoulou, C. (2012). Ventilation in European dwellings: A review. *Building and Environment*, *47*(1), 109–125. doi:10.1016/j.buildenv.2011.07.016

Dimitroulopoulou, C., Crump, D., Coward, S., Brown, B., Squire, R., Mann, H., … Ross, H. (2005). *Ventilation, air tightness, and indoor air quality in new homes*. Watford, UK: BRE Bookshop.

Emenius, G., Egmar, A. C., & Wickman, M. (1998). Mechanical ventilation protects one-storey single-dwelling houses against increased air humidity, domestic mite allergens and indoor pollutants in a cold climatic region. *Clinical and Experimental Allergy*, *28*(11), 1389–1396. doi:10.1046/j.1365-2222.1998.00408.x

Emenius, G., Svartengren, M., Korsgaard, J., Nordvall, L., Pershagen, G., & Wickman, M. (2004). Building characteristics, indoor air quality and recurrent wheezing in very young children (BAMSE). *Indoor Air*, *14*(1), 34–42. doi:10.1046/j.1600-0668.2003.00207.x

European Union. (2018). *Directive 2018/844 of the European parliament and of the council of 30 May 2018 amending directive 2010/31/EU on the energy performance of buildings and directive 2012/27/EU on energy efficiency, 2018 §*, Brussels, Belgium.

Farshad, F. F., Garber, J. D., & Lorde, J. N. (2000). Predicting temperature profiles in producing oil wells using artificial neural networks. *Engineering Computations*, *17*(6), 735–754. doi:10.1108/02644400010340651

Fletcher, R. (1980). *Practical methods of optimization*. Chichester: John Wiley&Sons.

Galvin, R., & Sunikka-Blank, M. (2017). Ten questions concerning sustainable domestic thermal retrofit policy research. *Building and Environment*, *118*, 377–388. doi:10.1016/j.buildenv.2017.03.007

Gładyszewska-Fiedoruk, K. (2013). Correlations of air humidity and carbon dioxide concentration in the kindergarten. *Energy and Buildings*, *62*, 45–50. doi:10.1016/j.enbuild.2013.02.052

The Government of Spain. (1979). *Royal decree 2429/79. Approving the basic building norm NBE-CT-79, about the thermal conditions in buildings*, Madrid, Spain.

The Government of Spain. (2013). *Royal decree 314/2006. Approving the Spanish technical building code CTE-DB-HE-1*, Madrid, Spain.

The Government of Spain. (2017). *Descriptive document reference climates (CTE-DB-HE)*, Madrid, Spain.

Gradeci, K., Labonnote, N., Time, B., & Köhler, J. (2017). Mould growth criteria and design avoidance approaches in wood-based materials – a systematic review.

Construction and Building Materials, *150*, 77–88. doi:10.1016/j.conbuildmat.2017.05.204

Haldi, F. (2015). Predicting the risk of moisture induced damages on the building envelope using stochastic models of building occupants' behaviour. *Energy Procedia*, *78*, 1377–1382. doi:10.1016/j.egypro.2015.11.157

Hägerhed-Engman, L., Bornehag, C. G., & Sundell, J. (2009). Building characteristics associated with moisture related problems in 8,918 Swedish dwellings. *International Journal of Environmental Health Research*, *19*(4), 251–265. doi:10.1080/09603120802527653

Hens, H. (2003). Mold in dwellings: Field studies in a moderate climate. In *Proceedings of the 24th AIVC conference and BETEC conference, ventilation, humidity control and energy* (pp. 12–14). Retrieved from http://www.kuleuven.be/bwf/projects/annex41/protected/data/KUL Apr 2006 Paper A41-T4-B-06-5.pdf

Holme, J., Hägerhed-Engman, L., Mattsson, J., Sundell, J., & Bornehag, C. G. (2010). Culturable mold in indoor air and its association with moisture-related problems and asthma and allergy among Swedish children. *Indoor Air*, *20*(4), 329–340. doi:10.1111/j.1600-0668.2010.00658.x

Hou, J., Zhang, Y., Sun, Y., Wang, P., Zhang, Q., Kong, X., & Sundell, J. (2018). Air change rates at night in northeast Chinese homes. *Building and Environment*, *132*(January), 273–281. doi:10.1016/j.buildenv.2018.01.030

Howden-Chapman, P., Saville-Smith, K., Crane, J., & Wilson, N. (2005). Risk factors for mold in housing: A national survey. *Indoor Air*, *15*(6), 469–476. doi:10.1111/j.1600-0668.2005.00389.x

International Organization for Standardization. (2012). *ISO 13788:2012 – hygrothermal performance of building components and building temperature to avoid critical surface humidity and interstitial condensation – calculation methods*, Geneva, Switzerland.

International Organization for Standardization. (2017). *ISO 10211:2017 – thermal bridges in building construction – heat flows and surface temperatures – detailed calculations*, Geneva, Switzerland.

Jacob, B., Ritz, B., Gehring, U., Koch, A., Bischof, W., Wichmann, H. E., & Heinrich, J. (2002). Indoor exposure to molds and allergic sensitization. *Environmental Health Perspectives*, *110*(7), 647–653. doi:10.1289/ehp.02110647

Jentsch, M. F., Bahaj, A. B. S., & James, P. A. B. (2008). Climate change future proofing of buildings-generation and assessment of building simulation weather files. *Energy and Buildings*, *40*(12), 2148–2168. doi:10.1016/j.enbuild.2008.06.005

Jentsch, M. F., James, P. A. B., Bourikas, L., & Bahaj, A. B. S. (2013). Transforming existing weather data for worldwide locations to enable energy and building performance simulation under future climates. *Renewable Energy*, *55*, 514–524. doi:10.1016/j.renene.2012.12.049

Kim, J., Kim, T., & Leigh, S. B. (2011). Double window system with ventilation slits to prevent window surface condensation in residential buildings. *Energy and Buildings*, *43*(11), 3120–3130. doi:10.1016/j.enbuild.2011.08.012

Klemm, A. J., Klemm, P., Rozniakowski, K., & Wojtatowicz, T. W. (2002a). Non-contact methods of measuring moisture concentration in external layers of building partitions: II – monitoring of the water vapour condensation on porous surfaces. *Building and Environment*, *37*(12), 1221–1232. doi:10.1016/S0360-1323(01)00124-X

Klemm, A. J., Klemm, P., Rozniakowski, K., & Wojtatowicz, T. W. (2002b). Non-contact methods of measuring moisture concentration in external layers of building partitions III – water vapour condensation on the cementitious surfaces. *Building and Environment*, *37*(12), 1233–1240. doi:10.1016/S0360-1323(01)00123-8

Koskinen, O. M., Husman, T. M., Meklin, T. M., & Nevalainen, A. I. (1999). The relationship between moisture or mould observations in houses and the state of health of their occupants. *European Respiratory Journal*, *14*(6), 1358–1362. doi:10.1183/09031936.99.14613639

Krus, M., Rosler, D., & Sedlbauer, K. (2006). New model for the hygrothermal calculation of condensate on the external building surface. In *Proceedings of third international building physics conference – research in building physics and building engineering* (pp. 27–31). Montreal: Concordia University.

Kumar, R., Aggarwal, R. K., & Sharma, J. D. (2013). Energy analysis of a building using artificial neural network: A review. *Energy and Buildings*, *65*(2), 352–358. doi:10.1016/j.enbuild.2013.06.007

Kurtz, F., Monzón, M., & López-Mesa, B. (2015). Energy and acoustics related obsolescence of social housing of Spain's post-war in less favoured urban areas. The case of Zaragoza. *Informes de La Construcción*, *67*(Extra-1), m021. doi:10.3989/ic.14.062

Levie, D., Kluizenaar de, Y., Hoes-van Oeffelen, E. C. M., Hofstetter, H., Janssen, S. A., Spiekman, M. E., & Koene, F. G. H. (2014). Determinants of ventilation behavior in naturally ventilated dwellings: Identification and quantification of relationships. *Building and Environment*, *82*, 388–399. doi:10.1016/j.buildenv.2014.09.008

Liu, J., Aizawa, H., & Yoshino, H. (2004). CFD prediction of surface condensation on walls and its experimental validation. *Building and Environment*, *39*(8 SPEC. ISS.), 905–911. doi:10.1016/j.buildenv.2004.01.015

Met Office Hadley Centre. (2016). *Met Office Hadley Centre for climate science and services*. Retrieved from http://www.metoffice.gov.uk/climate-guide/science/science-behind-climate-change/hadley

Orr, S. A., Young, M., Stelfox, D., Curran, J., & Viles, H. (2018). Wind-driven rain and future risk to built heritage in the United Kingdom: Novel metrics for characterising rain spells. *Science of the Total Environment*, *640–641*, 1098–1111. doi:10.1016/j.scitotenv.2018.05.354

Park, J. S., & Kim, H. J. (2012). A field study of occupant behavior and energy consumption in apartments with mechanical ventilation. *Energy and Buildings*, *50*, 19–25. doi:10.1016/j.enbuild.2012.03.015

Peci López, F., & Ruiz de Adana Santiago, M. (2015). Sensitivity study of an opaque ventilated façade in the winter season in different climate zones in Spain. *Renewable Energy*, *75*, 524–533. doi:10.1016/j.renene.2014.10.031

Pereira, C., de Brito, J., & Silvestre, J. D. (2018). Contribution of humidity to the degradation of façade claddings in current buildings. *Engineering Failure Analysis*, *90*(October 2017), 103–115. doi:10.1016/j.engfailanal.2018.03.028

Platt, S. D., Martin, C. J., Hunt, S. M., & Lewis, C. W. (2009). Damp housing, mould growth, and symptomatic health

state. *BMJ*, *298*(6689), 1673–1678. doi:10.1136/bmj.298.6689.1673

Pope, V. D., Gallani, M. L., Rowntree, P. R., & Stratton, R. a. (2000). The impact of new physical parametrizations in the Hadley Centre climate model: HadAM3. *Climate Dynamics*, *16*(2–3), 123–146. doi:10.1007/s003820050009

Rubel, F., & Kottek, M. (2010). Observed and projected climate shifts 1901-2100 depicted by world maps of the Köppen-Geiger climate classification. *Meteorologische Zeitschrift*, *19*(2), 135–141. doi:10.1127/0941-2948/2010/0430

Sánchez-García, D., Rubio-Bellido, C., Pulido-Arcas, J. A., Guevara-García, F. J., & Canivell, J. (2018). Adaptive comfort models applied to existing dwellings in Mediterranean climate considering globalwarming. *Sustainability (Switzerland)*, *10*(10). doi:10.3390/su10103507

Schweizer, C., Edwards, R. D., Bayer-Oglesby, L., Gauderman, W. J., Ilacqua, V., Juhani Jantunen, M., … Künzli, N. (2007). Indoor time-microenvironment-activity patterns in seven regions of Europe. *Journal of Exposure Science and Environmental Epidemiology*, *17*(2), 170–181. doi:10.1038/sj.jes.7500490

Sharpe, R. A., Bearman, N., Thornton, C. R., Husk, K., & Osborne, N. J. (2015). Indoor fungal diversity and asthma: A meta-analysis and systematic review of risk factors. *Journal of Allergy and Clinical Immunology*, *135*(1), 110–122. doi:10.1016/j.jaci.2014.07.002

Sharpe, R. A., Thornton, C. R., Nikolaou, V., & Osborne, N. J. (2015). Fuel poverty increases risk of mould contamination, regardless of adult risk perception & ventilation in social housing properties. *Environment International*, *79*, 115–129. doi:10.1016/j.envint.2015.03.009

Shin, M. S., Rhee, K. N., Lee, E. T., & Jung, G. J. (2018). Performance evaluation of CO2-based ventilation control to reduce CO2concentration and condensation risk in residential buildings. *Building and Environment*, *142*(June), 451–463. doi:10.1016/j.buildenv.2018.06.042

Sierra, F., Bai, J., & Maksoud, T. (2015). Impact of the simplification of the methodology used to assess the thermal bridge of the head of an opening. *Energy and Buildings*, *87*, 342–347. doi:10.1016/j.enbuild.2014.11.049

Singh, M. K., Mahapatra, S., & Teller, J. (2013). An analysis on energy efficiency initiatives in the building stock of Liege, Belgium. *Energy Policy*, *62*, 729–741. doi:10.1016/j.enpol.2013.07.138

Spanish Institute of Statistics. (2011). *Population and housing census*. Retrieved from https://www.ine.es/censos2011_datos/cen11_datos_resultados.htm#

Torres-Rivas, A., Palumbo, M., Haddad, A., Cabeza, L. F., Jiménez, L., & Boer, D. (2018). Multi-objective optimisation of bio-based thermal insulation materials in building envelopes considering condensation risk. *Applied Energy*, *224* (September 2017), 602–614. doi:10.1016/j.apenergy.2018.04.079

Urquhart, D. C. M. (1982). Condensation and mould growth in houses. *Batiment International, Building Research and Practice*, *10*(2), 88. doi:10.1080/09613218208551032

Woolliscroft, M. (1997). PH-97-8-3. Residential ventilation in the United Kingdom: An overview. In *ASHRAE transactions: Symposia* (Vol. 103, p. 706716), Atlanta, GA.